Applied Nanoscience (2020) 10:3149–3160
https://doi.org/10.1007/s13204-019-01039-9

ORIGINAL ARTICLE

Mathematical modeling and analysis of Cross nanofluid flow subjected to entropy generation

S. Z. Abbas[1,2] · W. A. Khan[1,3] · H. Sun[1] · M. Ali[2] · M. Irfan[4] · M. Shahzed[2] · F. Sultan[2]

Received: 15 February 2019 / Accepted: 9 April 2019 / Published online: 19 April 2019

Abstract
Here modeling and computations are performed to explore the aspects of entropy generation for magnetohydrodynamic (MHD) mixed convective flow of Cross nanoliquid. Heat transfer process comprises thermal radiation and Joule heating. Moreover, phenomenal aspect of current review is to consider the characteristics of activation energy. The idea of combined convective conditions and zero mass flux relation is introduced first time. The similarity transformation helps to simplify the complex model in the form of nonlinear PDEs into nonlinear ODEs. Numerical algorithm leads to solution computations. The numerical solutions of temperature, nanoparticle concentration fields, Nusselt number and coefficient of skin friction are exhibited via plots. It is noticed that radiation factor increases the thermal field and related layer thickness. Moreover, the obtained data reveal that profiles of Bejan number intensify for augmented values of radiation parameter. Intensifies

Keywords Cross nanoliquid · Magnetohydrodynamic (MHD) · Entropy generation · Viscous dissipation · Activation energy

List of symbols

u, v	Velocity components
x, y	Space coordinates
ρ_f	Density of fluid
ν	Kinematic viscosity
μ	Dynamic viscosity
n	Power law index
B_0	Uniform magnetic field strength
$(\rho c)_{\mathrm{f}}$	Heat capacity of fluid
τ	Ratio of heat capacity
$(\rho c)_{\mathrm{p}}$	Effective heat capacity
α	Thermal diffusivity
σ^{**}	Stefan–Boltzmann constant
D_{T}	Thermophoresis effect
k	Thermal conductivity
c_{p}	Specific heat capacity
k^*	Mean absorption coefficient
D_{B}	Brownian motion
T	Temperature
T_∞	Ambient temperature
C_∞	Ambient concentration
T_{w}	Surface temperature
k_{r}^2	Reaction rate
E_{a}	Activation energy
Γ	Time material constant
β^*	Ratio of viscosities
C	Concentration
m	Fitted rate constant
c	Dimensional constant
U_{w}	Stretching velocity
η	Dimensionless variable
We	Weissenberg number
Pr	Prandtl number
M	Magnetic parameter
Nr	Buoyancy ratio parameter
λ	Mixed convection parameter
R	Thermal radiation parameter
Nb	Brownian motion parameter
Nt	Thermophoresis parameter
Ec	Eckert number
Sc	Schmidt number
σ	Dimensionless reaction rate

✉ W. A. Khan
waqar_qau85@yahoo.com

[1] School of Mathematics and Statistics, Beijing Institute of Technology, Beijing 100081, China

[2] Department of Mathematics and Statistics, Hazara University, Mansehra 21300, Pakistan

[3] Department of Mathematics, Mohi-ud-Din Islamic University, Nerian Sharif, Azad Jammu and Kashmir 12010, Pakistan

[4] Department of Mathematics, Quaid-I-Azam University, Islamabad 44000, Pakistan

E	Dimensionless activation energy
δ	Temperature difference parameter
τ_w	Wall shear stress
q_w	Wall heat flux
f	Dimensionless velocities
θ	Dimensionless temperature
ϕ	Dimensionless concentration
N_G	Entropy generation rate
α_2	Dimensionless temperature ratio variable
α_1	Dimensionless concentration ratio variable
L	Diffusive variable
Br	Brinkman number
C_{fx}	Skin fraction
Nu_x	Local Nusselt number
Re_x	Local Reynolds number

Introduction

Among the intensifying challenges of current world, the effectiveness and efficiency of engineering applications are becoming more prominent. Energy depletion is one of the essential concerns in the modern word. To avoid the energy loss in transportation phenomena's, it is highly required to use efficient medium. Modern methodologies have paved the way to manufacture materials at nanoscale. Nanotechnology is the most dynamic area that fascinates the research community owing to their significant features and enabling the substantial enhancement in the performance of devices. Furthermore, outstanding characteristics of nanomaterials have contributed significantly in numerous industrial thermal exchange liquid improvements. Recently, meaningful work has been performed to produce innovative heat transfer liquid termed as nanoliquid. Nanoliquids possess higher thermal properties in comparison with base liquids. Choi (1995) was the first who established nanoliquids. Such liquids have the capability to enhance thermal conductivity and thermal performance of carrier liquids. Heat transfer improvement can be modified by type of number of submerged nanoparticles, material and shape of particle. Nanoliquids have large-scale utilization in industrial and technological processes such as nuclear reactor cooling, power generator, micro-reactors, melt-spinning, drying and cooling of papers, air planes and glass fiber technology. Nanoliquid mechanism includes numerous factors such as thermophoretic force, thermal diffusion, micro-convection, particle to particle coupling, Brownian movement and conduction which were investigated recently by several scientists. These scientists proved that nanoparticle Brownian movement is the leading factor that improves thermal characteristics and energy productivity of liquids. Some literature regarding nanoliquid flow has been studied. Sheikholeslami et al. (2014) studied the flow of CuO water nanofluid and transfer of heat considering the aspects of Lorentz forces. Khan and Khan (2014) reported heat sink–source aspects for 3D non-Newtonian nanofluid. Ellahi et al. (2015) examined the effect of nano-size particle for CO–H_2O over inverted vertical cone. Khan et al. (2016), Khan and Khan (2015, 2016) described properties of nanofluid by considering different non-Newtonian fluid models. Waqas et al. (2016) investigated the flow of micropolar liquid due to nonlinear stretched sheet with convective condition. Khan and Khan (2016) presented characteristics of Burgers fluid by considering features of nanomaterials. Sulochana et al. (2017) analyzed the consequences of thin din needle with joule heating. Hayat et al. (2017) worked on the effects of applied magnetic field on nanofluid flow due to exponential stretching sheet with effect of thermal radiation. Sheikholeslami and Shehzad (2017) explored properties of nanofluid by considering characteristics of Lorentz force. Some recent developments on nanofluid have been discussed in Refs. (Sheikholeslami and Shamlooei 2017; Sheikholeslami and Rokni 2017; Irfan et al. 2018; Hayat et al. 2018; Sheikholeslami et al. 2018; Gireesha et al. 2018; Mahanthesh et al. 2018; Sheikholeslami 2018a, b; Akbar and Khan 2016; Sheikholeslami and Shehzad 2018a, b; Sheikholeslami and Sadoughi 2018; Sheikholeslami and Seyednezhad 2018; Irfan et al. 2018, 2019; Khan et al. 2018; Sheikholeslami and Rokni 2018; ; 2019; Sheikholeslami et al. Sheikholeslami 2019a, b; Khan et al. 2019; Sheikholeslami et al. 2019; Sheikholeslami and Mahian 2019; Nematpour Keshteli and Sheikholeslami 2019).

A chemical reaction is a process (reversible/irreversible) that generates entropy. Many chemical reaction systems, homogeneous and heterogeneous, catalytic and non-catalytic, and single and multiple, are categorized with respect to their chemical and physical properties. The homogeneous reactions are uniform consisting a single phase space; it may be gas, liquid or solid. Unlike homogeneous reactions, the heterogeneous reactions are not uniform in nature. The homogeneous reaction can be the component of heterogeneous reaction. The homogeneous/heterogeneous mixture of chemical reaction system has received much attention from researchers due to its widespread applications in industrial process, biochemical system and catalysis. Khan et al. (2016, 2017) examined feature chemical process for non-Newtonian fluids. Mahanthesh et al. (2017) revealed properties of nanofluid for vertical plate. Impact of chemical processes and modified heat flux relation was studied by Sohail et al. (2017). Ramesh et al. (2018) considered chemical processes and zero mass flux relation for Maxwell nanoliquid. Irfan et al. (2018) studied aspects of chemical processes for Carreau fluid with heat sink–source and variable conductivity. Non-Newtonian nanofluid with aspects of activation and chemical processes was investigated by Khan et al. (2018).

Irfan et al. (2019) discussed the heterogeneous–homogeneous reactions for Oldroyd-B fluid.

Keeping in prospect of beforehand mentioned published works, it is detected that entropy generation aspects for Cross fluid have not yet been examined. Therefore, the main theme of existing consideration is to colloidal and entropy generation aspects for Cross material. Transportation of heat is examined through heat sink–source aspects. Effects of viscous dissipation and thermal radiation are also taken into account. Physical interpretation of involved parameters in modeled problem is inspected via graphs.

Formulation

Here aspects of activation energy and entropy generation minimization for radiative flow of Cross nanomaterial in the presence of Lorentzís forces are considered. Mathematical formulation is based on thermophoresis and Brownian motion. Moreover, viscous dissipation and radiation features in energy expression are taken into account. Arrhenius activation energy is also a part of discussion. Governing problem for the present situation is listed as

$$\frac{\partial u}{\partial x}+\frac{\partial v}{\partial y}=0, \tag{1}$$

$$\begin{aligned} u\frac{\partial u}{\partial x}+v\frac{\partial u}{\partial y} &= \upsilon\frac{\partial^2 u}{\partial y^2}\left[\beta^*+(1-\beta^*)\frac{1}{1+(\Gamma\frac{\partial u}{\partial y})^n}\right] \\ &+\upsilon(1-\beta^*)\frac{\partial u}{\partial y}\frac{\partial}{\partial y}\left[\frac{1}{1+(\Gamma\frac{\partial u}{\partial y})^n}\right] \\ &-\frac{\sigma^* B_0^2}{\rho_f}u+g\left[A_1\left(T-T_\infty\right)+A_2\left(C-C_\infty\right)\right], \end{aligned} \tag{2}$$

$$\begin{aligned} u\frac{\partial T}{\partial x}+v\frac{\partial T}{\partial y} &= \frac{v}{c_p}\left(\frac{\partial u}{\partial y}\right)^2\left[\beta^*+(1-\beta^*)\frac{1}{1+(\Gamma\frac{\partial u}{\partial y})^n}\right] \\ &+\alpha\frac{\partial^2 T}{\partial y^2}+\tau\frac{D_T}{T_\infty}\left(\frac{\partial T}{\partial y}\right)^2 \\ &+\tau D_B\frac{\partial C}{\partial y}\frac{\partial T}{\partial y}-\frac{1}{(\rho c)_f}\frac{\partial q_w}{\partial y}, \end{aligned} \tag{3}$$

$$u\frac{\partial C}{\partial x}+v\frac{\partial C}{\partial y}=\frac{D_T}{T_\infty}\frac{\partial^2 T}{\partial y^2}+D_B\frac{\partial^2 C}{\partial y^2} - k_r^2\left(C-C_\infty\right)\left(\frac{T}{T_\infty}\right)^m\exp\left(-\frac{E_a}{\kappa T}\right), \tag{4}$$

with

$$u=U_w=cx,\ v=0,\ T=T_w,\ D_B\frac{\partial C}{\partial y}+\frac{D_T}{T_\infty}\frac{\partial T}{\partial y}=0 \text{ at } y=0, \tag{5}$$

$$u\to 0,\ T\to T_\infty,\ \ C\to C_\infty \text{ as } y\to\infty. \tag{6}$$

Considering

$$\begin{aligned} &\eta=y\sqrt{\frac{c}{v}},\ v=-\sqrt{cv}f(\eta),\ u=cxf'(\eta) \\ &\theta(\eta)=\frac{T_\infty-T}{T_\infty-T_w},\ \varphi(\eta)=\frac{C-C_\infty}{C_\infty}. \end{aligned} \tag{7}$$

One has

$$\begin{aligned} &\left[\beta^*\left\{1+\left(Wef''\right)^n\right\}^2+(1-\beta^*)\left\{1+(1-n)\left(Wef''\right)^n\right\}\right]f''' \\ &-\left[1+\left(Wef''\right)^n\right]^2\left[f'^2+ff''+\lambda(\theta+Nr\phi)\right]=0, \end{aligned} \tag{8}$$

$$\left(1+\frac{4}{3}R\right)\theta'' + \Pr\left[f\theta'+Nb\theta'\phi'+Nt\theta'^2+Ecf''^2\beta^*+(1-\beta^*)\frac{Ecf''^2}{1+\left(Wef''\right)^n}\right]=0 \tag{9}$$

$$\phi''+Sc\left[f\phi'+\frac{Nt}{Nb}\theta''-\sigma(1+\delta\theta)^m\phi\exp\left(-\frac{E}{1+\delta\theta}\right)\right]=0 \tag{10}$$

$$f(0)=0,\ \ f'(0)-1=0,\ \ f'(\infty)\to 0, \tag{11}$$

$$\theta(0)=1,\ \ \theta(\infty)\to 0 \tag{12}$$

$$Nb\phi'(0)=-Nt\theta'(0),\ \phi(\infty)\to 0. \tag{13}$$

Non-dimensional form of variables occurring in Eqs. (8)–(13) is given below:

$$M = \frac{\sigma^* B_0^2}{\rho_f c_f}, Pr = \frac{\nu}{\alpha}, R = \frac{4\sigma^{**} T_\infty^3}{k^* k}, Nb = \frac{\tau D_B (C_\infty)}{\upsilon},$$
$$Nt = \frac{\tau D_T (T_w - T_\infty)}{\nu T_\infty}, \sigma = \frac{kr^2}{c},$$
$$Ec = \frac{c^2 x^2}{c_p (T_w - T_\infty)}, We = \sqrt{\frac{\Gamma^2 c^3 x^2}{\nu}}, \tag{14}$$
$$Sc = \frac{\nu}{D_B}, E = \frac{E_a}{\kappa T_\infty}, \delta = \frac{T_w - T_\infty}{T_\infty}, \beta^* = \frac{\mu_\infty}{\mu_0}.$$

Physical quantities

Mathematically, the expression of Nusselt and Sherwood numbers (C_{fx}, Nu_x) in dimensional form is:

$$C_{fx} = \frac{\tau_w}{\rho_f U_w^2}, \tag{15}$$

$$Nu_x = \frac{x q_w}{k(T_w - T_\infty)}, \tag{16}$$

where

$$\tau_w = \mu \frac{\partial u}{\partial y}\left[\beta^* + (1-\beta^*)\frac{1}{1 + \left(\Gamma \frac{\partial u}{\partial y}\right)^n}\right], \tag{17}$$

$$q_w = -k\frac{\partial T}{\partial y} - \frac{16\sigma^{**} T_\infty^3}{3k^*}\frac{\partial T}{\partial y}. \tag{18}$$

From Eqs. (17) and (18), one obtains:

$$C_{fx} Re_x^{1/2} = \left[\beta^* + (1-\beta^*)\frac{1}{1 + \left(Wef''(0)\right)^n}\right] f''(0), \tag{19}$$

$$Nu_x Re_x^{-1/2} = -\left[1 + \frac{4}{3}R\right]\theta'(0), \tag{20}$$

where $Re_x = \frac{xU_w}{\nu}$.

Analysis of entropy generation

Mathematical relation of volumetric entropy generation for Cross fluid in dimensional form is expressed as

$$S_G = \frac{k}{T_\infty^2}\left[1 + \frac{16\sigma^* T_\infty^3}{3kk^*}\left(\frac{\partial T}{\partial y}\right)^2\right] + \frac{\mu}{T_\infty}\left(\frac{\partial u}{\partial y}\right)^2\left[\beta^* + (1-\beta^*)\frac{1}{1 + \left(\Gamma\frac{\partial u}{\partial y}\right)^n}\right] + \frac{\sigma^* B_0^2 u^2}{T_\infty} + \frac{RD}{C_\infty}\left(\frac{\partial C}{\partial y}\right)^2 + \frac{RD}{T_\infty}\left(\frac{\partial T}{\partial y}\frac{\partial C}{\partial y}\right). \tag{21}$$

In dimensionless, one has:

$$N_G = \alpha_1\left[1 + \frac{4}{3}R\right]\theta'^2 + Br\left[\beta^* + \frac{(1-\beta^*)}{1 + (Wef'')^n}\right]f''^2 + MBrf'^2 + \frac{\alpha_2}{\alpha_1}L\phi'^2 + L\theta'\phi', \tag{22}$$

where

$$Br = \frac{\mu U_w^2}{\kappa \Delta T}, \quad \alpha_1 = \frac{\Delta T}{T_\infty}, \quad N_G = \frac{\nu T_\infty S_G}{\kappa c \Delta T}, \quad L = \frac{RC_\infty D}{k}. \tag{23}$$

Be is expressed as

$$Be = \frac{\text{Entropy generation subject to heat and mass transfer}}{\text{Total entropy generation}}, \tag{24}$$

$$Be = \frac{\alpha_1\left[1 + \frac{4}{3}R\right]\theta'^2 + \frac{\alpha_2}{\alpha_1}L\phi'^2 + L\theta'\phi'}{\alpha_1\left[1 + \frac{4}{3}R\right]\theta'^2 + Br\left[\beta^* + \frac{1-\beta^*}{1+\left(Wef''\right)^n}\right]f''^2 + MBrf'^2 + \frac{\alpha_2}{\alpha_1}L\phi'^2 + L\theta'\phi'}. \tag{25}$$

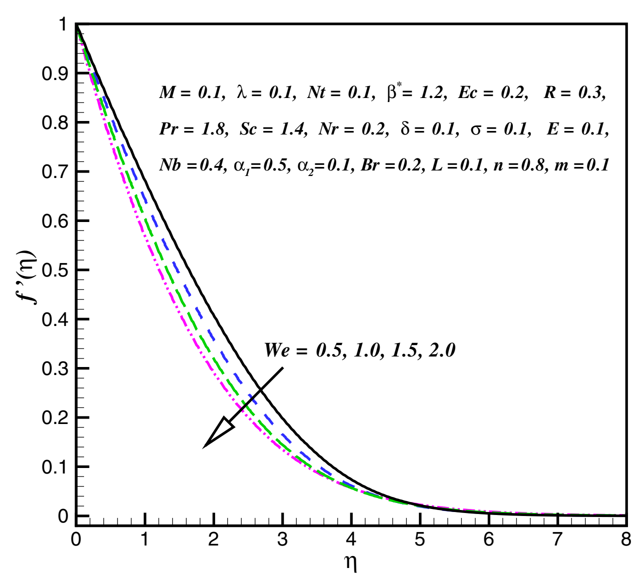

Fig. 1 f' impact for different We

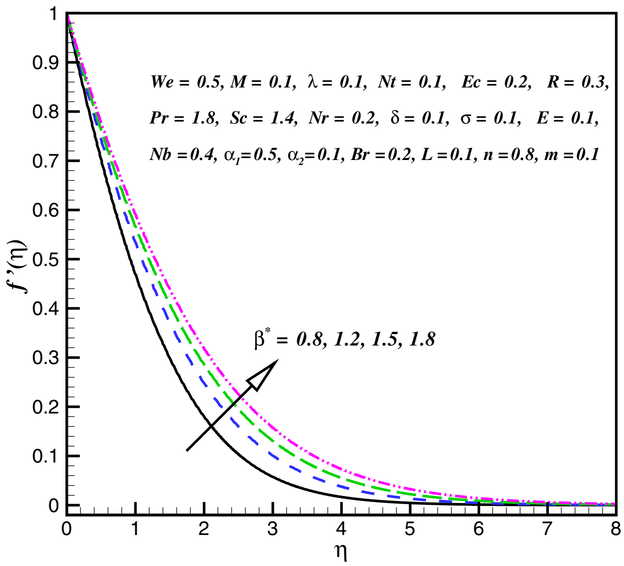

Fig. 2 f' impact for different β^*

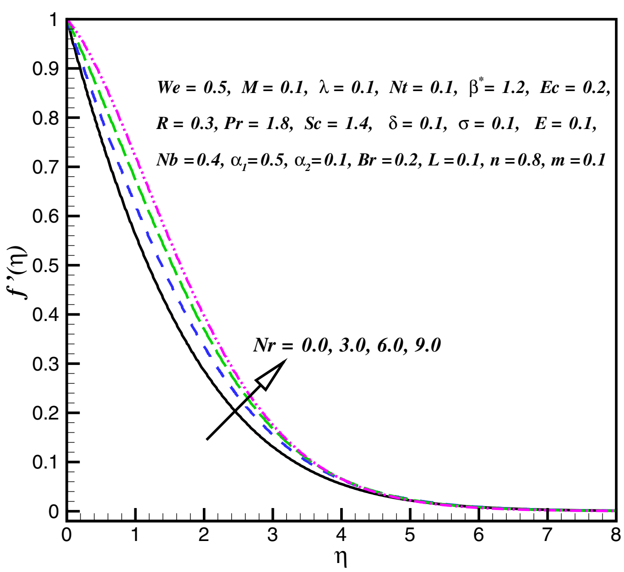

Fig. 3 f' impact for different Nr

Discussion

Here our emphasis is to scrutinize features of entropy generation for Cross nanofluid. Transportation of heat is analyzed in the presence of heat sink–source and radiation aspects. Set of Eqs. (8)–(13), (22) and (15) along with associated conditions are tackled numerically via MATLAB tool bvp4c.

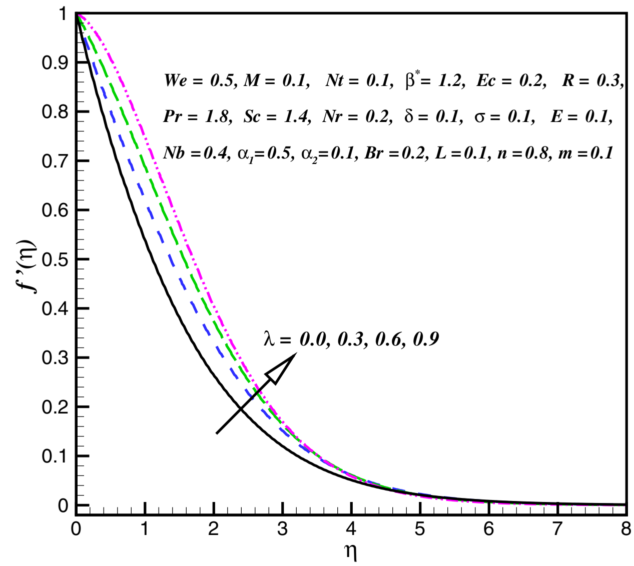

Fig. 4 f' impact for different λ

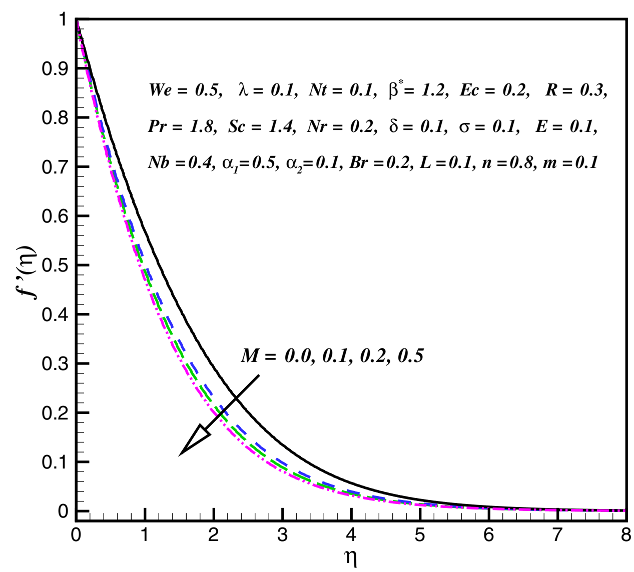

Fig. 5 f' impact for different M

Nanofluid velocity profiles

Figure 1 reveals the features of We on f'. We observed from obtained data that f' enhances via larger We for shear thinning liquid. Figure 2 is plotted to scrutinize the impact of β^* on f'. We observed that f' enhances for higher estimation of β^*. Analysis for features of Nr on f' is addressed in Fig. 3. Here f' is increasing function for larger Nr. The curve of f' for different values of λ is investigated in Fig. 4.

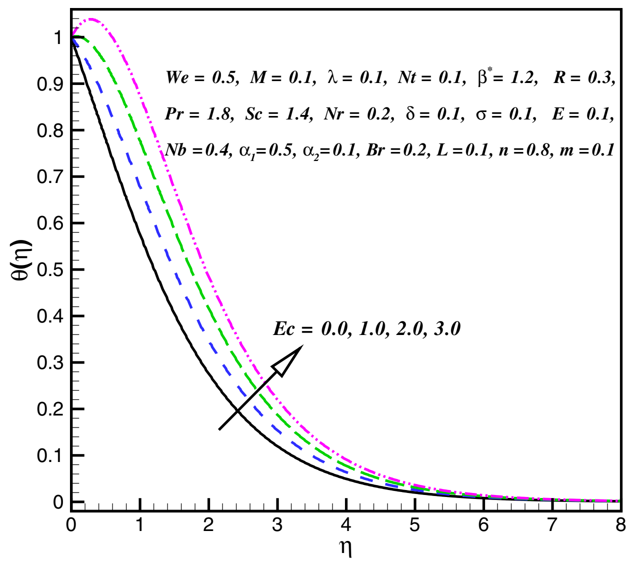

Fig. 6 θ impact for different Ec

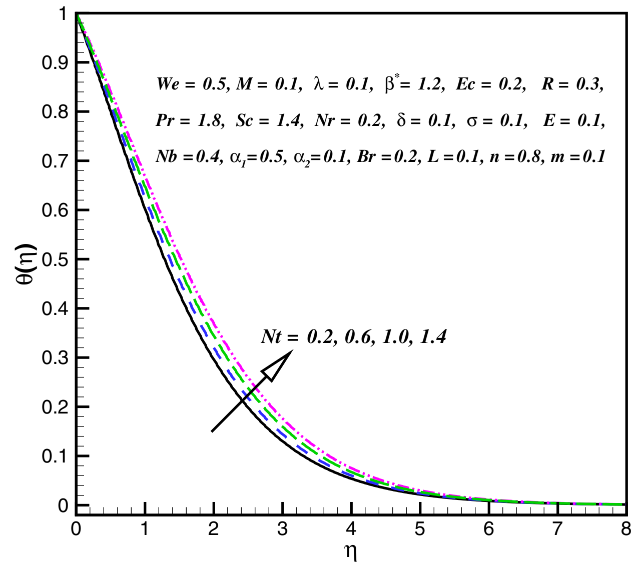

Fig. 8 θ impact for different Nt

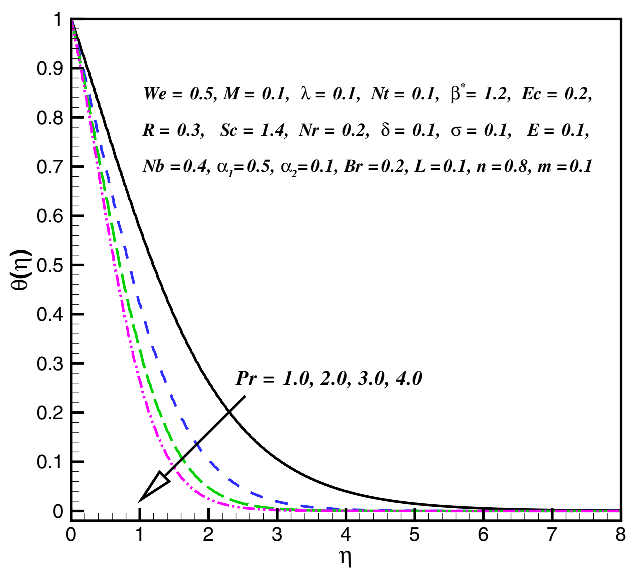

Fig. 7 θ impact for different Pr

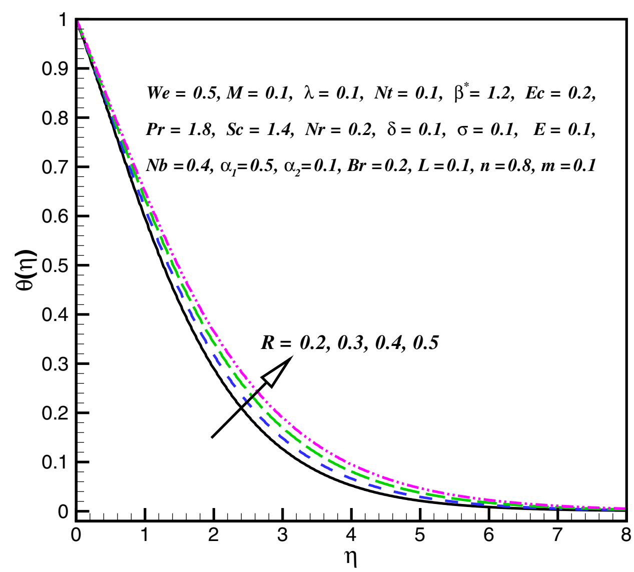

Fig. 9 θ impact for different R

We noticed an improvement in f' subject to larger λ. Physically, the enhancement in buoyancy forces yields higher liquid velocity. The impact of M on f' is presented in Fig. 5. Here f' decays via larger M. The liquid velocity is much smaller in hydromagnetic case when compared with hydrodynamic case. It is due to the fact that Lorentz force becomes stronger when M increases. Therefore, stronger Lorentz force creates resistance to transport phenomenon which is accountable for diminishment in the velocity f'.

Nanofluid temperature profiles

Figure 6 interprets θ variation for Ec. Here θ augments when Ec is increased. Relation between the flow of enthalpy difference and KE (kinetic energy) is called Eckert number. It elaborates change of KE (kinetic energy) into internal energy by work done versus the viscous liquid stresses. The larger Ec causes loss of heat from the plate to the liquid, i.e. cooling of the plate. In other words, larger energy dissipation produces higher liquid temperature. Features of Pr on θ is exhibited in Fig. 7. Here θ decays when Pr is increased. In

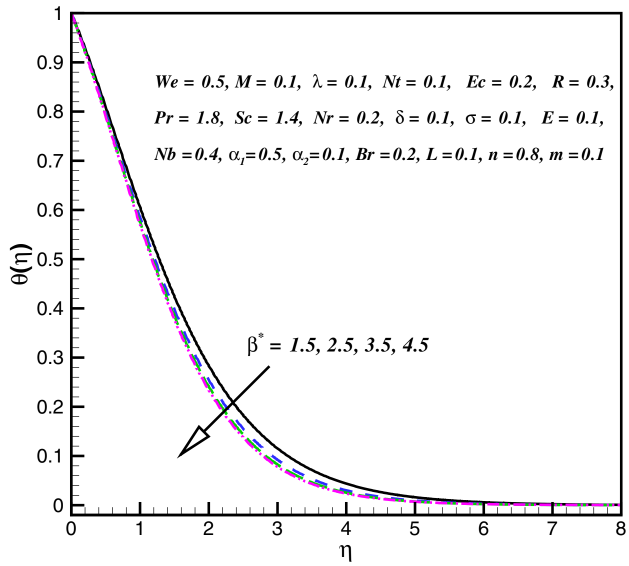

Fig. 10 θ impact for different β^*

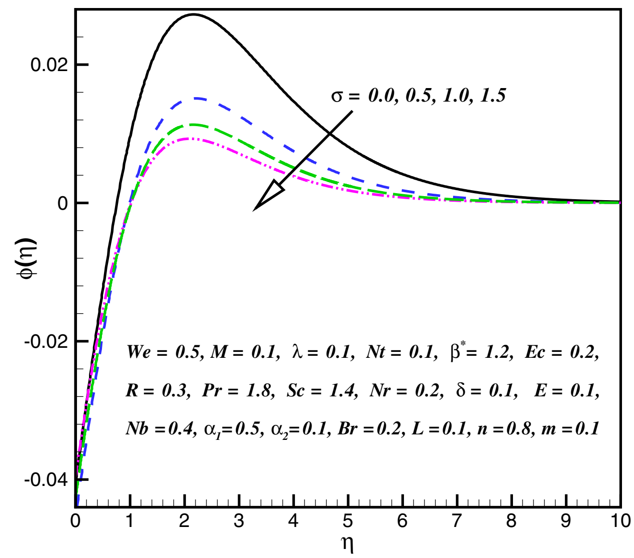

Fig. 12 φ impact for different σ

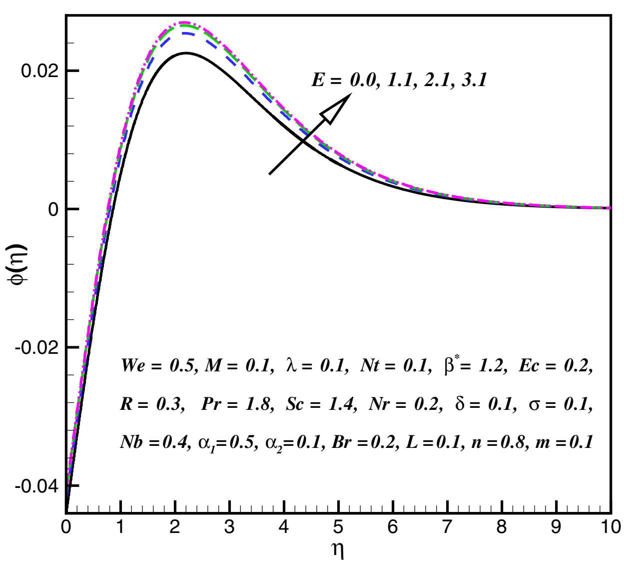

Fig. 11 φ impact for different E

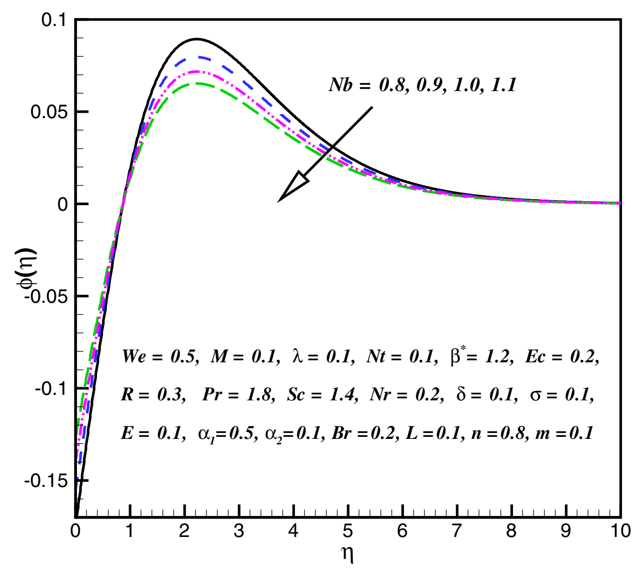

Fig. 13 φ impact for different N_{b}

fact, larger Pr reduces the thermal diffusivity which accordingly decay liquid temperature. Figure 8 portrays the impact of Nt on θ. Clearly, larger Nt yields higher θ. Physically, small number of particles are pulled away from hot region to cold one in thermophoresis phenomenon. Hence, a large number of nanomaterials are moved away from the heated region which inflates the liquid temperature. The role of R on θ is explored in Fig. 9. Clearly, a rise in R augments θ. Physically, radiation process produces more heat in the working liquid; therefore, θ and related thermal layer thickness enhance. Figure 10 is plotted to examine the impact of β^* on θ. We observed that θ decreases for higher estimation of β^*.

Nanofluid concentration profiles

Figure 11 depicts the behavior of E for ϕ. It is examined that the term $\exp\left(-\frac{E_{\mathrm{a}}}{\kappa T}\right)$ decreases for higher estimation of E_{a}. This eventually generates a chemical reaction due to which ϕ improves. Figure 12 is plotted to examine the impact of σ

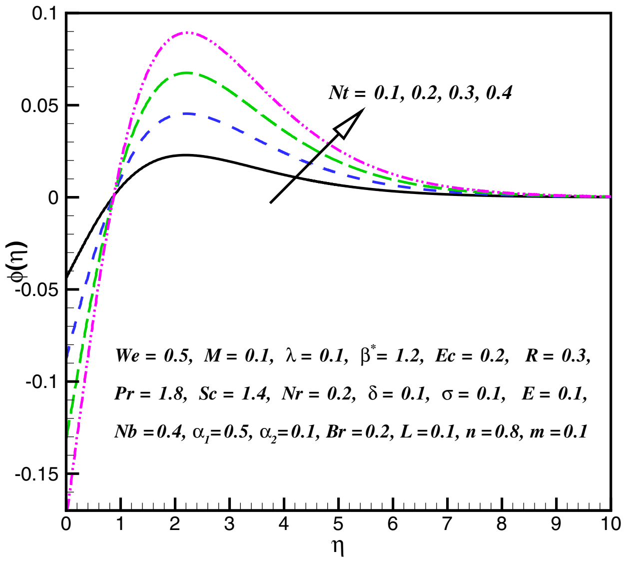

Fig. 14 φ impact for different N_t

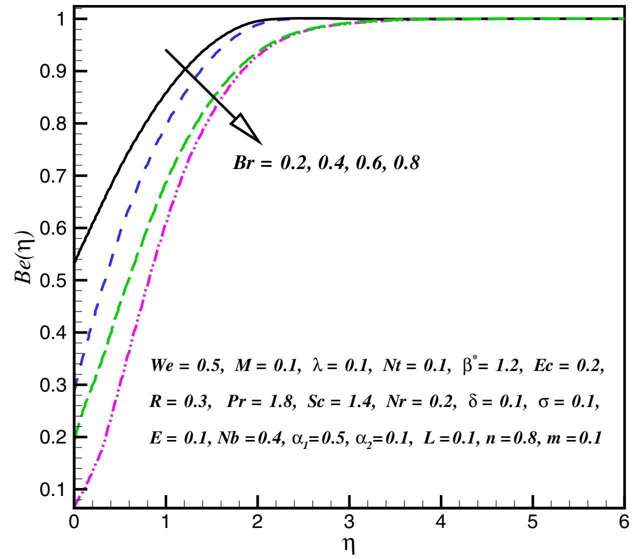

Fig. 16 *Be* impact for different *Br*

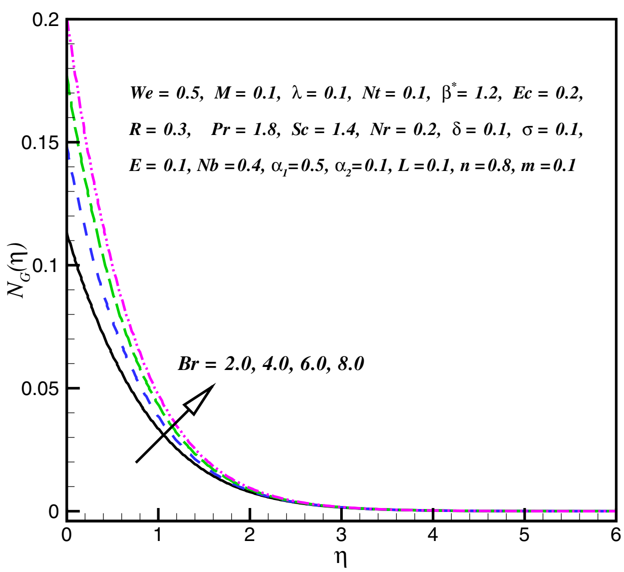

Fig. 15 N_G impact for different *Br*

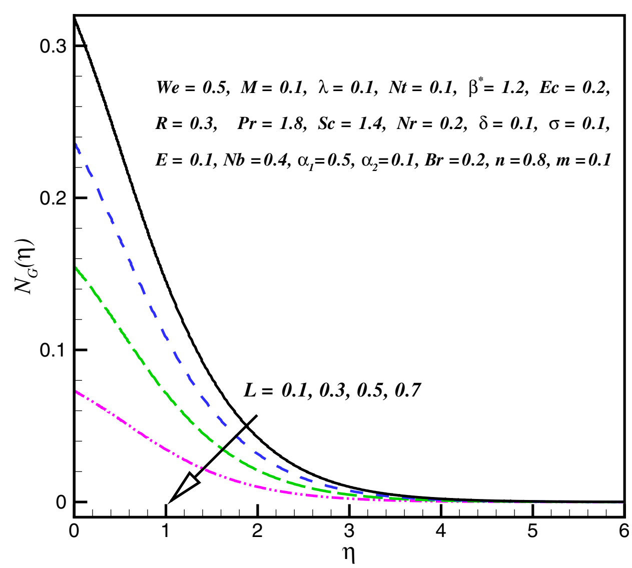

Fig. 17 N_G impact for different *L*

on ϕ. We observed that ϕ enhances for higher estimation of σ. Actually, the consumption of reactive species decays rapidly for larger σ. The impacts of N_t and N_b on ϕ are interpreted in Figs. (13 and 14). For larger N_t and thickness of nanoparticles, concentration boundary layer escalates. Actually, thermophoretic force increases for higher estimation of N_t due to which nanoparticles moves from higher to lower temperature and boosts up (See Fig. 13). Moreover, ϕ and its associated concentration layer reduce when N_b is increased (See Fig. 14).

Entropy generation rate and Bejan number

Figures 15 and 16 depict the salient features of *Br* on N_G and *Be*. In fact, Brinkman number *Br* has characteristic to propagate heat by viscous flowing liquid to heat transport through molecular conduction, e.g. in polymer processing. Heat transport via molecular conduction is much greater than heat propagation via viscous effects. Consequently, movement of liquid particles generates more heat between the adjacent layers. It enhances the entropy and system disorderness (see Fig. 15). Figure 16 displays that *Be* decays

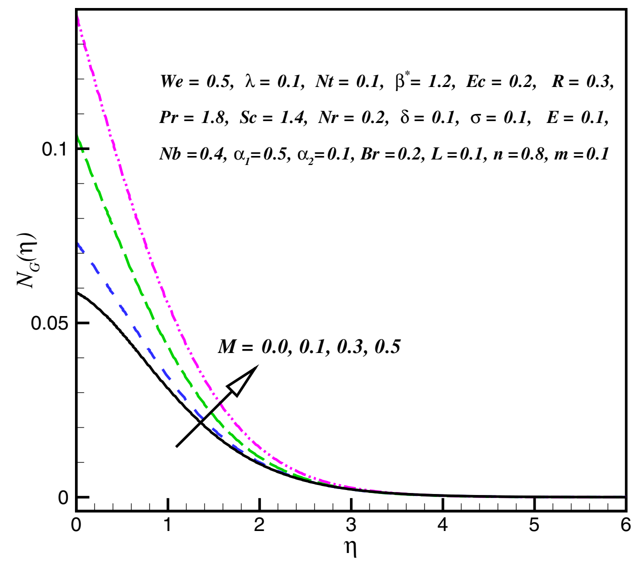

Fig. 18 N_G impact for different M

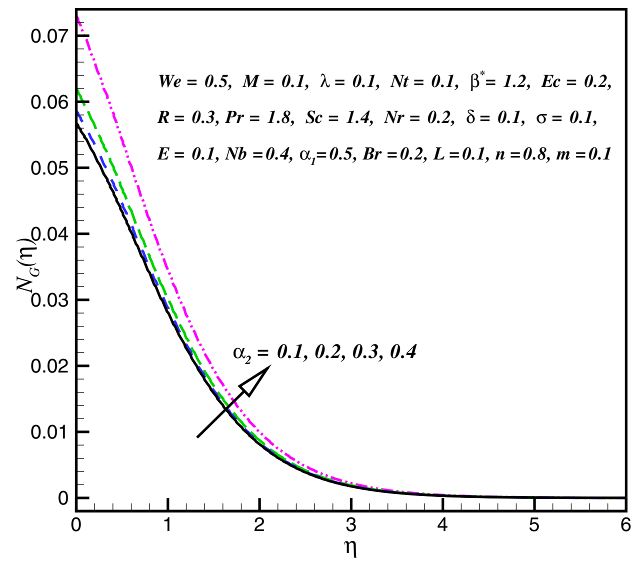

Fig. 20 N_G impact for different α_2

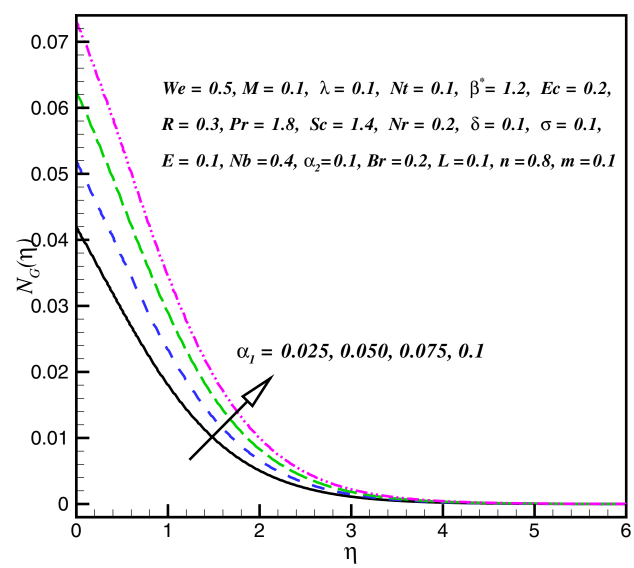

Fig. 19 N_G impact for different α_1

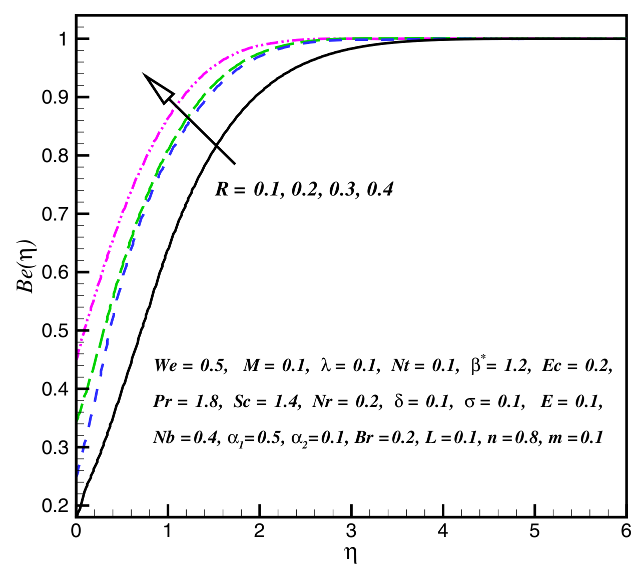

Fig. 21 Be impact for different R

via larger Br. It is due to the fact that larger Br corresponds to increase in entropy rate which decays the Be. Figure 17 reports the impact of L on N_G. Clearly, N_G shows a decreasing trend for L. Figure 18 discloses the characteristics of M on N_G. Here, it is noticed that N_G augments when M is increased. Physically, rise in M creates greater Lorentz force due to which resistance in liquid flow increases and N_G enhances. Figure 19 Illustrates the characteristics of α_1 on N_G. Here, N_G enhances via larger α_1. Physically, liquid temperature increases for larger α_1 which accordingly enhances entropy generation rate. The curves of α_2 on N_G is displayed in Fig. 20. It is evaluated that liquid concentration increases when α_2 is increased and consequently N_G enhances. Figures 21 reveals the impact of R on Be. Here, Be enhances when R is augmented.

Features of drag force and heat transportation rate

Table 1 portrays the influences of We, λ, n, Nr, M and β^* on surface drag force. Here, surface drag force enhances via larger We and M, whereas it decays for larger λ, n, Nr and β^*. Table 2 points out the features of several embedded

Table 1 Computational outcomes of surface drag forces ($Re^{1/2}C_{fx}$)

We	λ	*n*	*Nr*	*M*	β^*	$Re^{1/2}C_{fx}$
0.5	0.1	0.1	0.2	0.1	1.5	1.42215
1.0	–	–	–	–	–	1.865175
1.5	–	–	–	–	–	2.143035
2.0	0.2	–	–	–	–	2.144928
–	0.4	–	–	–	–	1.788143
–	0.6	–	–	–	–	1.456623
–	–	0.3	–	–	–	1.913039
–	–	0.5	–	–	–	1.371898
–	–	0.7	–	–	–	0.840992
–	–	–	0.5	–	–	2.299866
–	–	–	0.7	–	–	2.276837
–	–	–	1.0	–	–	2.242216
–	–	–	–	0.4	–	1.141962
–	–	–	–	0.8	–	0.7213266
–	–	–	–	1.2	–	0.3134904
–	–	–	–	–	2.0	1.604637
–	–	–	–	–	2.5	1.776579
–	–	–	–	–	3.0	1.931452

Table 2 Computational outcomes for rate of heat transfer ($Re^{-1/2}Nu$)

Ec	β^*	*Pr*	*R*	*Nt*	*Nb*	$Nu_xRe_x^{-1/2}$
0.0	1.2	1.0	0.3	0.1	0.4	0.563821
0.2	–	–	–	–	–	0.348475
0.3	–	–	–	–	–	0.24225
0.4	1.5	–	–	–	–	0.202715
–	1.8	–	–	–	–	0.18716
–	2.0	–	–	–	–	0.17747
–	–	1.2	–	–	–	0.209459
–	–	1.4	–	–	–	0.235816
–	–	1.6	–	–	–	0.279022
–	–	–	0.6	–	–	0.288555
–	–	–	0.9	–	–	0.34932
–	–	–	1.2	–	–	0.404428
–	–	–	–	0.2	–	0.209816
–	–	–	–	0.4	–	0.190105
–	–	–	–	0.6	–	0.171909
–	–	–	–	–	0.5	0.199896
–	–	–	–	–	0.7	0.162627
–	–	–	–	–	0.9	0.12888

physical parameters on heat transfer rate. It is examined that heat transfer rate increases via larger *Pr* and *R*, whereas it decays for larger $Ec, \beta^*,\ Nt$ and *Nb*.

Conclusions

This research scrutinizes the influence of entropy generation minimization for Cross nanoliquid with Joule heating. Thermal radiation, thermophoresis and Brownian movement are taken into account for modeling and analysis. This research leads to following outcomes:

- Liquid velocity is decreasing function for larger *We*.
- Increments in R_d intensifies liquid temperature.
- Thermal and nanoparticle profiles are boosted via larger Nt .
- Stronger Lorentz's force leads to higher entropy generation rate while decays for Bejan number.
- Larger Brinkman gives rise to entropy generation rate in comparison with Bejan number.
- Surface drag force reduces for larger magnetic parameter.
- Heat transfer rate enhances via larger Prandtl number and radiative parameter when compared with Eckert number and thermophoretic parameter.

References

Akbar NS, Khan ZH (2016) Effect of variable thermal conductivity and thermal radiation with CNTS suspended nanofluid over a stretching sheet with convective slip boundary conditions: Numerical study. J Mol Liq 222:279–286

Nematpour Keshteli A, Sheikholeslami M (2019) Nanoparticle enhanced PCM applications for intensification of thermal performance in building: a review. J Mol Liq 274:516–533

Choi SUS (1995) Enhancing thermal conductivity of fluids with nanoparticles. ASME Int Mech Eng 66:99–105

Ellahi R, Hassan M, Zeeshan A (2015) Shape effects of nanosize particles in Cu-H2O nanofluid on entropy generation. Int J Heat Mass Transf 81:449–456

Gireesha BJ, Mahanthesh B, Thammanna GT, Sampathkumar PB (2018) Hall effects on dusty nanofluid two-phase transient flow past a stretching sheet using KVL model. J Mol Liq 256:139–147

Hayat T, Rashid M, Imtiaz M, Alsaedi A (2017) MHD effects on a thermo-solutal stratified nanoáuid flow on an exponentially radiating stretching sheet. J Appl Mech Tech Phys. https://doi.org/10.1134/s0021894417020043

Hayat T, Kiyani MZ, Alsaedi A, Khan MI, Ahmad I (2018) Mixed convective three-dimensional flow of Williamson nanofluid subject to chemical reaction. Int J Heat Mass Transf 127:422–429

Irfan M, Khan M, Khan WA, Ayaz M (2018a) Modern development on the features of magnetic field and heat sink/source in Maxwell nanofluid subject to convective heat transport. Phys Lett A 382(30):1992–2002

Irfan M, Khan M, Khan WA (2018b) Behavior of stratifications and convective phenomena in mixed convection flow of 3D Carreau nanofluid with radiative heat flux. J Braz Soc Mech Sci Eng 40:521. https://doi.org/10.1007/s40430-018-1429-5

Irfan M, Khan M, Khan WA (2018c) Interaction between chemical species and generalized Fourier's law on 3D flow of Carreau fluid with variable thermal conductivity and heat sink/source: a numerical approach. Results Phys 10:107–117

Irfan M, Khan M, Khan WA, Ahmad L (2019a) Influence of binary chemical reaction with Arrhenius activation energy in MHD nonlinear radiative flow of unsteady Carreau nanofluid: dual solutions. Appl Phys A 125:179. https://doi.org/10.1007/s00339-019-2457-4

Irfan M, Khan M, Khan WA (2019b) Impact of homogeneous–heterogeneous reactions and non-Fourier heat flux theory in Oldroyd-B fluid with variable conductivity. J Braz Soc Mech Sci Eng 41:135. https://doi.org/10.1007/s40430-019-1619-9

Khan WA, Khan M (2014) Three-dimensional flow of an Oldroyd-B nanofluid towards stretching surface with heat generation/absorption. PLoS One 9(8):e10510

Khan M, Khan WA (2015) Forced convection analysis for generalized Burgers nanofluid flow over a stretching sheet. AIP Adv 5:107138. https://doi.org/10.1063/1.4935043

Khan M, Khan WA (2016a) MHD boundary layer flow of a power-law nanofluid with new mass flux condition. AIP Adv 6:025211. https://doi.org/10.1063/1.4942201

Khan M, Khan WA (2016b) Steady flow of Burgers nanofluid over a stretching surface with heat generation/absorption. J Braz Soc Mech Sci Eng 38(8):2359–2367

Khan M, Khan WA, Alshomrani AS (2016a) Non-linear radiative flow of three-dimensional Burgers nanofluid with new mass flux effect. Int J Heat Mass Transf 101:570–576

Khan WA, Alshomrani AS, Khan M (2016b) Assessment on characteristics of heterogeneous-homogenous processes in three-dimensional flow of Burgers fluid. Results Phys 6:772–779

Khan WA, Irfan M, Khan M, Alshomrani AS, Alzahrani AK, Alghamdi MS (2017) Impact of chemical processes on magneto nanoparticle for the generalized Burgers fluid. J Mol Liq 234:201–208

Khan WA, Alshomrani AS, Alzahrani AK, Khan M, Irfan M (2018a) Impact of autocatalysis chemical reaction on nonlinear radiative heat transfer of unsteady three-dimensional Eyring-Powell magneto-nanofluid flow. Pramana J Phys 91:63. https://doi.org/10.1007/s12043-018-1634-x

Khan MI, Qayyum S, Hayat T, Khan MI, Alsaedi A, Khan TA (2018b) Entropy generation in radiative motion of tangent hyperbolic nanoáuid in presence of activation energy and nonlinear mixed convection. Phys Lett A 382:2017–2026

Khan WA, Sultan F, Ali M, Shahzad M, Khan M, Irfan M (2019) Consequences of activation energy and binary chemical reaction for 3D flow of Cross-nanofluid with radiative heat transfer. J Braz Soc Mech Sci Eng 41:4. https://doi.org/10.1007/s40430-018-1482-0

Mahanthesh B, Gireesha BJ, Athira PR (2017) Radiated flow of chemically reacting nanoliquid with an induced magnetic field across a permeable vertical plate. Results Phys 7:2375–2383

Mahanthesh B, Gireesha BJ, Shehzad SA, Rauf A, Kumar PBS (2018) Nonlinear radiated MHD flow of nanoliquids due to a rotating disk with irregular heat source and heat flux condition. Phys B Condens Matter 537:98–104

Ramesh GK, Shehzad SA, Hayat T, Alsaedi A (2018) Activation energy and chemical reaction in Maxwell magneto-nanoliquid with passive control of nanoparticle volume fraction. J Braz Soc Mech Sci Eng. https://doi.org/10.1007/s40430-018-1353-8

Sheikholeslami M (2018a) Numerical approach for MHD Al_2O_3-water nanofluid transportation inside a permeable medium using innovative computer method. Comput Methods Appl Mech Eng. https://doi.org/10.1016/j.cma.2018.09.042

Sheikholeslami M (2018b) New computational approach for exergy and entropy analysis of nanofluid under the impact of Lorentz force through a porous media. Comput Methods Appl Mech Eng. https://doi.org/10.1016/j.cma.2018.09.044

Sheikholeslami M (2019a) New computational approach for exergy and entropy analysis of nanofluid under the impact of Lorentz force through a porous media. Comput Methods Appl Mech Eng 344:319–333

Sheikholeslami M (2019b) Numerical approach for MHD Al2O3-water nanofluid transportation inside a permeable medium using innovative computer method. Comput Methods Appl Mech Eng 344:306–318

Sheikholeslami M, Mahian O (2019) Enhancement of PCM solidification using inorganic nanoparticles and an external magnetic

field with application in energy storage systems. J Clean Prod 215:963–977
Sheikholeslami M, Rokni HB (2017) Numerical modeling of nanofluid natural convection in a semi annulus in existence of Lorentz force. Comput Methods Appl Mech Eng 317:419–430
Sheikholeslami M, Rokni HB (2018) Numerical simulation for impact of Coulomb force on nanofluid heat transfer in a porous enclosure in presence of thermal radiation. Int J Heat Mass Transf 118:823–831
Sheikholeslami M, Sadoughi MK (2018) Simulation of CuO-water nanofluid heat transfer enhancement in presence of melting surface. Int J Heat Mass Transf 116:909–919
Sheikholeslami M, Seyednezhad M (2018) Simulation of nanofluid flow and natural convection in a porous media under the influence of electric field using CVFEM. Int J Heat Mass Transf 120:772–781
Sheikholeslami M, Shamlooei M (2017) Fe3O4–H2O nanofluid natural convection in presence of thermal radiation. Int J Hydrogen Energy 42(9):5708–5718
Sheikholeslami M, Shehzad SA (2017) Magnetohydrodynamic nanofluid convective flow in a porous enclosure by means of LBM. Int J Heat Mass Transf 113:796–805
Sheikholeslami M, Shehzad SA (2018a) Simulation of water based nanofluid convective flow inside a porous enclosure via non-equilibrium model. Int J Heat Mass Transf 120:1200–1212
Sheikholeslami M, Shehzad SA (2018b) Numerical analysis of Fe3O4–H2O nanofluid flow in permeable media under the effect of external magnetic source. Int J Heat Mass Transf 118:182–192
Sheikholeslami M, Bandpy MG, Ellahi R, Zeeshan A (2014) Simulation of MHD CuO-water nanofluid flow and convective heat transfer considering Lorentz forces. J Magn Mag Mat 369:69–80
Sheikholeslami M, Jafaryar M, Shafee A, Li Z (2018) Investigation of second law and hydrothermal behavior of nanofluid through a tube using passive methods. J Mol Liq 269:407–416
Sheikholeslami M, Rizwan-ul Haq, Shafee A, Li Z (2019a) Heat transfer behavior of nanoparticle enhanced PCM solidification through an enclosure with V shaped fins. Int J Heat Mass Transf 130:1322–1342
Sheikholeslami M, Gerdroodbary MB, Moradi R, Shafee A, Li Z (2019b) Application of neural network for estimation of heat transfer treatment of Al2O3-H2O nanofluid through a channel. Comput Methods Appl Mech Eng 344:1–12
Sohail A, Khan WA, Khan M, Shah SIA (2017) Consequences of non-Fourier's heat conduction relation and chemical processes for viscoelastic liquid. Results Phys 7:3281–3286
Sulochana C, Ashwinkumar GP, Sandeep N (2017) Joule heating effect on a continuously moving thin needle in MHD Sakiadis flow with thermophoresis and Brownian moment. Eur Phys J Plus. https://doi.org/10.1140/epjp/i2017-11633-3
Waqas M, Farooq M, Khan MI, Alsaedi A, Hayat T, Yasmeen T (2016) Magnetohydrodynamic (MHD) mixed convection flow of micropolar liquid due to nonlinear stretched sheet with convective condition. Int J Heat Mass Transf 102:766–772